Geochemistry Geophysics Geosystems G3
AN ELECTRONIC JOURNAL OF THE EARTH SCIENCES
Published by AGU and the Geochemical Society

Article
Volume 8, Number 2
13 February 2007
Q02005, doi:10.1029/2006GC001403
ISSN: 1525-2027

Identifying and removing noise from the Monterey ocean bottom broadband seismic station (MOBB) data

David Dolenc, Barbara Romanowicz, and Robert Uhrhammer
Seismological Laboratory, University of California, 215 McCone Hall #4760, Berkeley, California 94720, USA (dolenc@seismo.berkeley.edu)

Paul McGill
Monterey Bay Aquarium Research Institute, Moss Landing, California 95039, USA

Doug Neuhauser
Seismological Laboratory, University of California, 215 McCone Hall #4760, Berkeley, California 94720, USA

Debra Stakes
Cuesta College, San Luis Obispo, California 93403, USA

[1] When compared to quiet land stations, the very broadband Monterey ocean bottom seismic station (MOBB) shows increased long-period background as well as signal-generated noise. Both sources of noise are unavoidable in shallow ocean bottom installations, and postprocessing is required to remove them from seismic observations. The long-period background noise observed for periods longer than 20 s is mainly due to infragravity waves and ocean currents. The shorter-period signal-generated noise, on the other hand, is due to reverberations of the seismic waves in the shallow sedimentary layers as well as in the water layer. We first present the steps that were taken prior to and during the instrument deployment to minimize instrument generated noise as well as to avoid noise due to water flow around the instrument. We then present results from two postprocessing methods that can be used to remove the long-period background noise, which both utilize the ocean bottom pressure signal locally recorded on a differential pressure gauge (DPG). One consists of subtracting the locally recorded ocean bottom pressure from the vertical seismic acceleration signal. In this case the frequency-independent scale factor is linearly estimated from the data. The other one makes use of the transfer function between the vertical seismic and pressure signal to predict the vertical component deformation signal. The predicted signal is then removed from the vertical seismic data in either frequency or time domain. We also present two methods that can be used to remove the signal-generated noise. One employs the empirical transfer function constructed from MOBB data and nearby land station data that do not show the signal-generated noise. The other one uses a synthetic transfer function computed by modeling the response of shallow layers at the MOBB location. Using either of the two transfer functions, most of the signal-generated noise can be removed from the MOBB data by deconvolution.

Components: 6406 words, 13 figures.

Keywords: ocean bottom seismology; seismic noise; ocean bottom seismic stations.

Index Terms: 4294 Oceanography: General: Instruments and techniques; 4299 Oceanography: General: General or miscellaneous; 7299 Seismology: General or miscellaneous.

Received 28 June 2006; **Revised** 4 November 2006; **Accepted** 20 November 2006; **Published** 13 February 2007.

Dolenc, D., B. Romanowicz, R. Uhrhammer, P. McGill, D. Neuhauser, and D. Stakes (2007), Identifying and removing noise from the Monterey ocean bottom broadband seismic station (MOBB) data, *Geochem. Geophys. Geosyst.*, *8*, Q02005, doi:10.1029/2006GC001403.

1. Introduction

[2] The Monterey ocean bottom broadband station (MOBB) was installed in April 2002, 40 km offshore in the Monterey Bay, at a water depth of 1000 m [*McGill et al.*, 2002; *Uhrhammer et al.*, 2002; *Romanowicz et al.*, 2003, 2006] and has been continuously operating in the last 4 years, through a collaborative effort between the Monterey Bay Aquarium Research Institute (MBARI) and the Berkeley Seismological Laboratory (BSL).

[3] The MOBB is located west of the San Gregorio Fault, one of the major faults of the San Andreas Fault System, in a region characterized by diverse topography. A wide, gently sloping continental shelf is found to the north, the 1500 m deep Monterey Canyon is just south of the MOBB, and a narrow shelf is present in the Monterey Bay and further to the south (Figure 1). The MOBB includes a 3-component Guralp CMG-1T broadband seismometer that is sensitive to ground vibrations over a wide frequency range, from 50 Hz to 2.8 mHz (360 s). The seismometer is mounted in a titanium pressure vessel, which is placed inside a 53-cm diameter $\times$ 61-cm deep cylindrical PVC caisson, buried in the ocean floor. The seismometer is connected to a recording and battery package that are installed in 1181 kg galvanized steel trawl-resistant ocean bottom mound, located about 11 m from the seismometer. Collocated are a differential pressure gauge (DPG) [*Cox et al.*, 1984] and a current meter, which measures ocean bottom current speed and direction. The station is autonomous and the data are, on average, retrieved every three months using the MBARI's remotely operated vehicle Ventana [*Romanowicz et al.*, 2003, 2006]. Efforts are underway to connect MOBB to the MARS fiber-optic cable (Monterey Accelerated Research System; http://www.mbari.org/mars). The data will then be retrieved continuously and in real-time and will be completely integrated in the northern California earthquake monitoring system operated jointly by the Berkeley Seismological Laboratory and the U.S. Geological Survey at Menlo Park. The data are currently available, after retrieval, from the Northern California Earthquake Data Center (NCEDC; http://www.ncedc.org/ncedc).

2. Instrument Testing and Deployment

[4] Before and during the initial deployment of the MOBB package in Monterey Bay, a number of steps were taken to minimize the instrument generated background noise as well as the noise induced by water flow around the seismometer. Prior to deployment, the seismometer system was extensively tested at BSL to minimize the long-period noise due to the sensitivity of the instrument to air movement within the titanium pressure vessel [*Uhrhammer et al.*, 2003]. The space between the walls of the pressure vessel and the seismometer package was insulated by multiple layers of Mylar space blanket. The space between the top of the seismometer and the bottom of the top-end cap of the pressure vessel was filled with a 2 inches thick urethane foam plug wrapped in Mylar. These steps provided insulation as well as reduced the air volume inside the pressure vessel. The remaining space was filled with argon gas. By insulating the top and sides of the cylindrical pressure vessel, but not the bottom, the $\sim$2.2 Watt power dissipation of the sensor produced a stable stratification of the argon gas. These steps significantly reduced noise that was observed on all three components in the 10–100 s period range, when convective air currents within the pressure vessel were allowed (Figure 2).

[5] During the deployment, the titanium pressure vessel with the seismometers was placed inside the PVC caisson buried in the ocean floor. Previous experiments [e.g., *Sutton et al.*, 1981; *Duennebier and Sutton*, 1995] showed that it is important to minimize water flow around the seismometer. To prevent noise from water circulation within the caisson, and similarly to the previous temporary MOISE experiment [*Romanowicz et al.*, 1998], tiny glass beads (0.8 mm diameter) were poured into the PVC caisson to completely cover the pressure vessel. The seismometer package is now buried at least 10 cm beneath the seafloor. To avoid the noise that could result from forces from the ocean bottom currents on the cable that connects

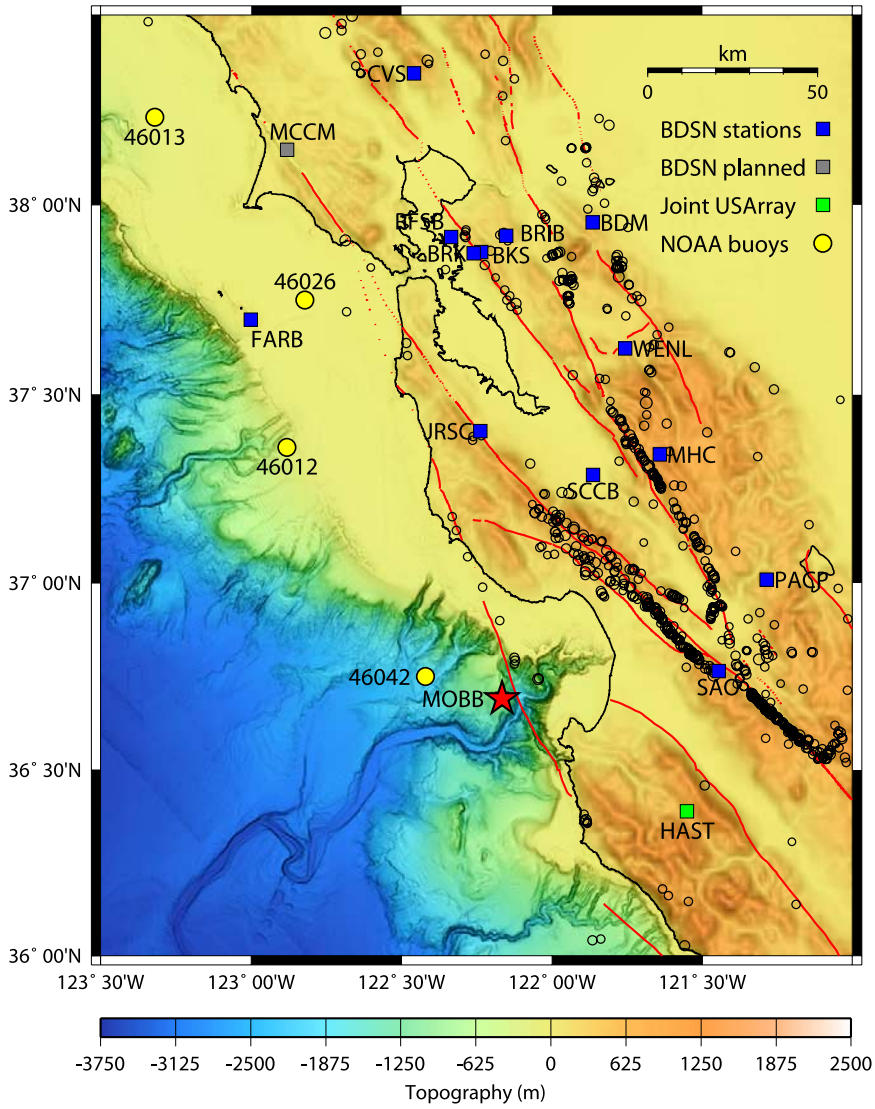

Figure 1. Locations of the MOBB (red) and the BDSN seismic stations (blue) shown against the seafloor and land topography. Background seismicity (ANSS catalog, 1968–2006, M3.5+) is shown in black. Locations of the NOAA buoys closest to the MOBB are shown in yellow. Fault lines from the California Division of Mines and Geology database are shown in red.

the seismometer with the recording package, the cable was immobilized by steel "wickets" that were inserted into the sediment.

[6] The steps described above minimized the noise that could be generated by the flow of air around the seismometers and by the flow of water around the pressure vessel housing the seismometers. By burying the seismometer package in the seafloor, immobilizing the cable, and placing the trawl-resistant mound at some distance from the seismometers, the noise from the eddies that could be generated from either of these units was minimized. The remaining long-period background noise observed at MOBB is primarily due to pressure forcing from infragravity ocean waves [*Dolenc et al.*, 2005].

3. Observations

[7] Many local, regional, and teleseismic events during the past 4 years have shown that strong events are well recorded (Figure 3). But for most events, additional processing is needed to improve the signal-to-noise ratio.

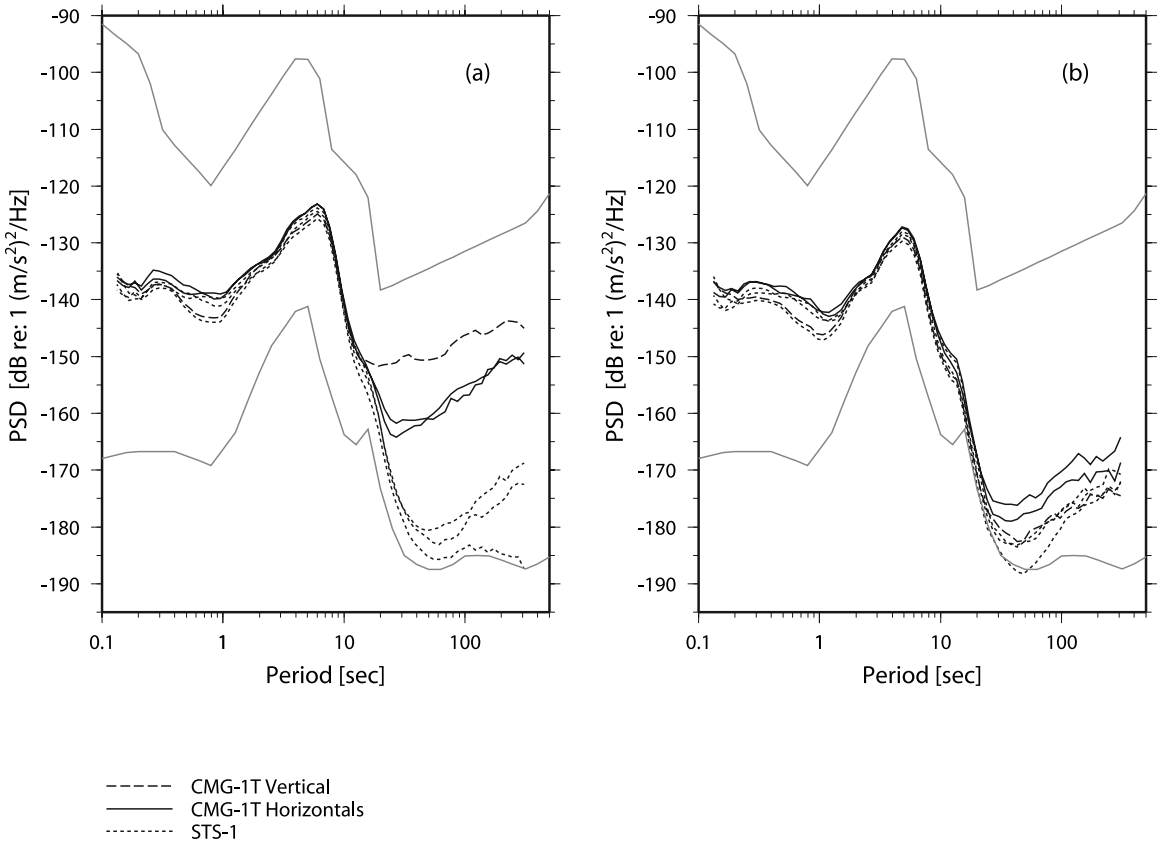

Figure 2. Comparison of the background noise power spectral density (PSD) from the CMG-1T ocean bottom seismometer and the STS-1 sensors. The titanium pressure vessel with the CMG-1T sensor was placed next to the STS-1 sensors inside the Byerly Seismographic Vault, the location of the BDSN station BKS. Shown are results for the CMG-1T vertical (large dashed) and the two horizontal components (solid) prior to installing the insulation and purging with argon gas (left) and after (right). The results for the three STS-1 components are shown for comparison (dotted). The CMG-1T PSD levels are within ~5 dB of the STS-1 PSD levels at long periods. The fact that CMG-1T and STS-1 PSD track each other over a wide range of periods also indicates that the CMG-1T calibration and transfer functions are correct. The USGS high- and low-noise models for land stations are shown in gray [*Peterson*, 1993].

3.1. Infragravity Waves

[8] Infragravity waves are ocean surface waves in the frequency band between 0.002 and 0.05 Hz. Results from a previous study [*Dolenc et al.*, 2005] showed that infragravity waves are a strong and always present source of long-period noise at the MOBB. A comparison of the power spectral density (PSD) at MOBB and three other BDSN land stations is shown in Figure 4 for a recent time period. Station SAO is the closest land station, station FARB is located on the Farallon Islands (see Figure 1), and station YBH is one of the quietest BDSN stations, located 560 km north of MOBB. Results for a quiet and for a stormy day are shown for the vertical (top) and for one horizontal component (E–W, bottom). Results for the two horizontal components were similar. The quiet and stormy day were selected on the basis of the spectral wave density (SWD) measured at the nearby NOAA buoy 46042 (Figure 1). Four hours of data were used in the calculation and there were no significant earthquakes recorded during the two time periods. The results show that a noise "hump" for periods between 20 and 200 s is observed on a quiet day for the MOBB vertical component data, but not for the land station data. The observed peak at MOBB is stronger and wider (periods 20–500 s) on a stormy day, when it can also be observed at the Farallon Islands station FARB. The fact that only linear waves with wave numbers comparable or smaller than the inverse of the water depth can generate a detectable pressure signal at the seafloor [*Webb*, 1998] results in the

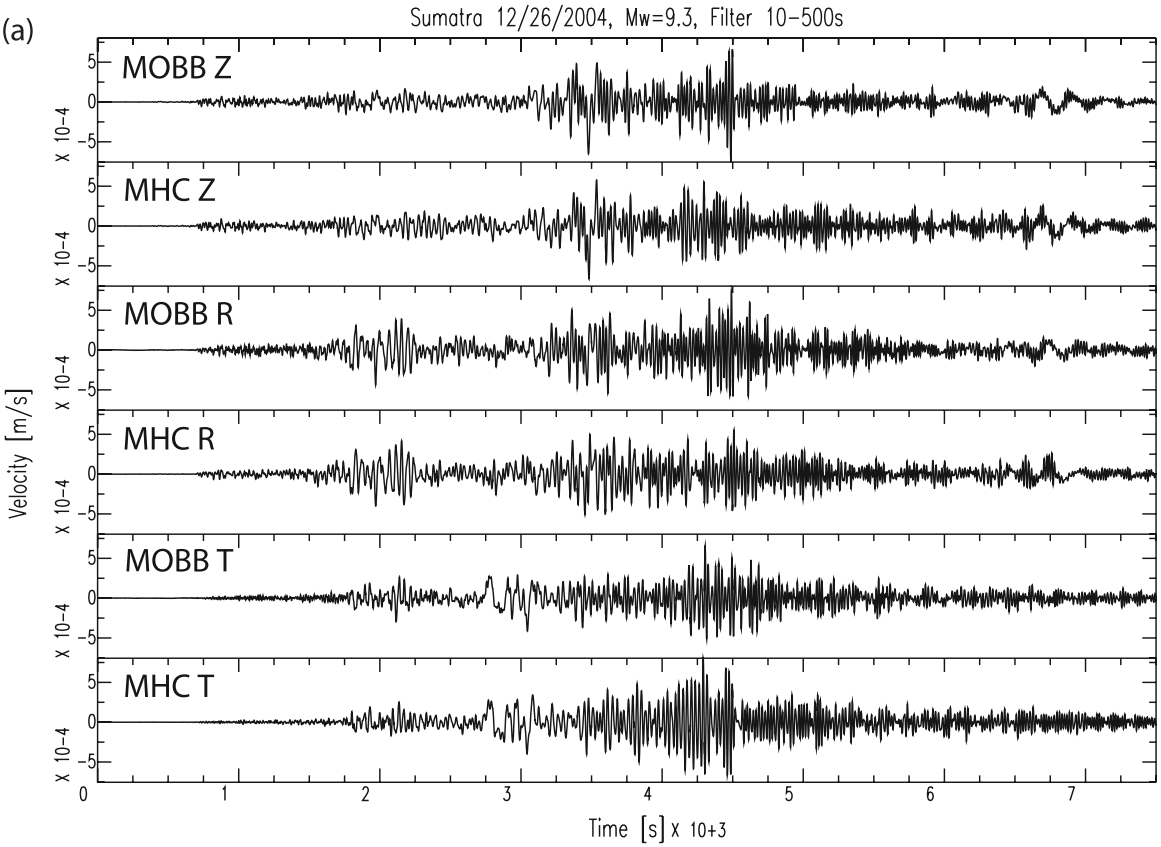

Figure 3. (a) Comparison of the great Sumatra M_w 9.3 26 December 2004 earthquake recorded at MOBB and MHC. Vertical, radial, and transverse components are shown. Waveforms were band-pass filtered between 10 and 500 s. Shown time window is 125 min long. (b) Comparison of the Rayleigh waves recorded on the vertical component at MOBB and MHC. Waveforms were band-pass filtered between 125 and 300 s. Shown time window is 13.9 hours long. (c) Comparison of the Love waves observed on the transverse component at MOBB and MHC. Waveforms were band-pass filtered between 125 and 300 s. Shown time window is 13.9 hours long.

sharp short-period cutoff observed at 20 s in the spectrum for the vertical MOBB component on a stormy day. On the horizontal components, the peak for periods longer than 20 s is observed at MOBB on a stormy day, but not on a quiet day, indicating that this signal is primarily generated by vertical pressure on the seafloor.

[9] The signal at the island station FARB on a stormy day is even stronger than at MOBB and it extends all the way to 1000 s, suggesting a combination of direct atmospheric effects (tilt) and conversion of infragravity waves to horizontal elastic motion. Our recent analyses of the relation between the short-period ocean waves and infragravity wave noise observed at the ocean bottom broadband stations offshore California, Oregon, and Washington [*Dolenc et al.*, 2005; *Dolenc*, 2006] suggest that the infragravity waves are generated close to the shore. The Farallon Islands are located not only close to the shore, but also on the continental shelf (see Figure 1), where hydrodynamic filtering [*Kinsman*, 1984] is weak due to shallow water depth, resulting in a strong infragravity waves pressure signal at the seafloor. Interaction of the ocean currents with the Farallon Islands should also contribute significantly to the long-period noise on the horizontal components. The observation that the long-period noise observed at the station FARB is stronger on the E-W than on the N-S component [*Romanowicz et al.*, 2006] suggests that the strongest tidal currents flow perpendicular to the shoreline, similarly to what we observed at the MOBB [see *Romanowicz et al.*, 2006, Figure 10].

[10] The shape of the noise spectra in the infragravity wave band measured at MOBB agrees with

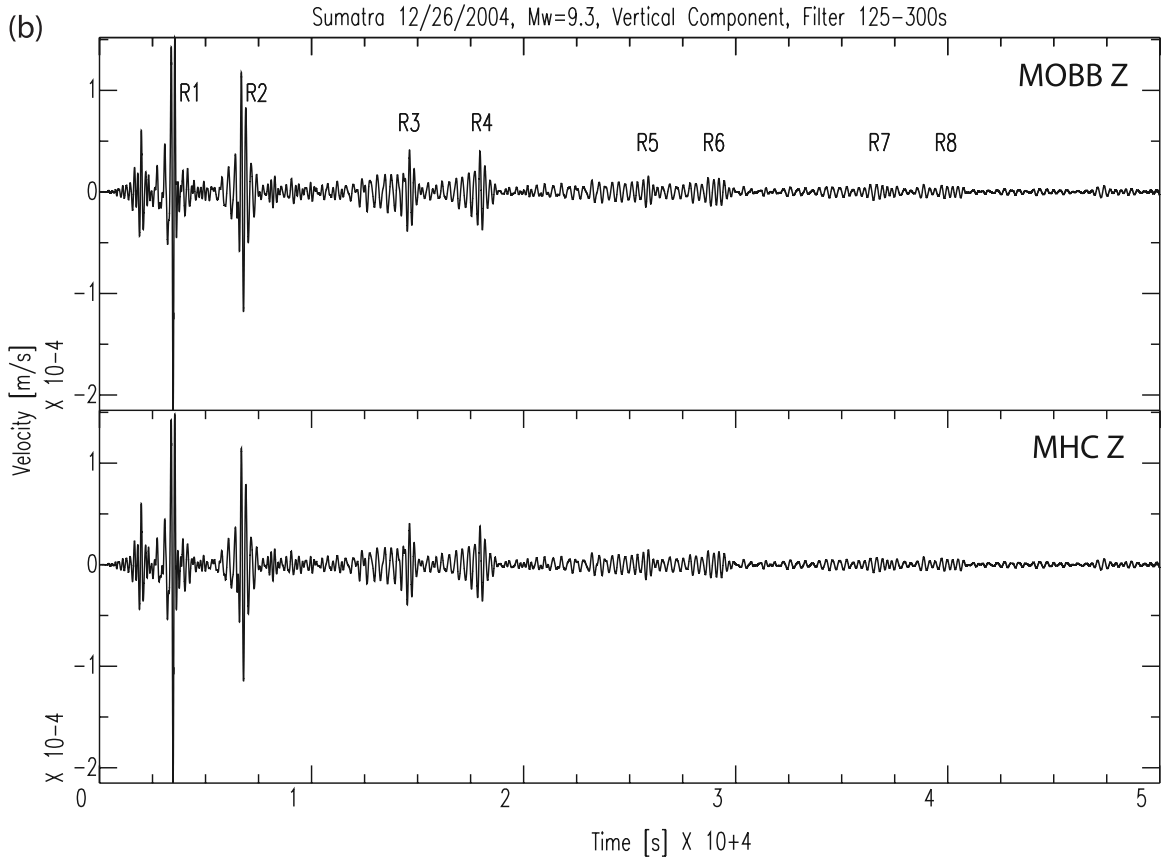

Figure 3. (continued)

theoretical predictions [*Araki et al.*, 2004] as well as with observations from other shallow buried seismometer deployments [*Stephen et al.*, 2003; *Araki et al.*, 2004].

[11] In the microseisms band, the two narrow peaks are observed between 1 and 10 s on a quiet day. These are two of the three peaks that are often observed in the spectra from the sites in the Pacific and are associated with the large storms in the Southern Ocean for the low-frequency peak, and with the local storms in the North Pacific for the main peak [*Webb*, 1998].

3.2. Reverberations of Seismic Waves in Sedimentary Layers

[12] The other type of noise observed at MOBB is signal-generated noise. It is due to reverberations of seismic waves in the shallow sedimentary layers and is particularly strong following the arrival of sharp and strong phases that are often characteristic of large deep events. An example of the signal-generated noise observed at MOBB is shown in Figure 5, where we compare the vertical component records at stations MOBB, FARB, JRSC, and SAO for the 565 km deep M_w 7.1 Fiji Islands earthquake of 15 July 2004. The waveforms in the 0.03 to 0.08 Hz passband show the arrivals of the P, pP, and PP phases, which look similar for all four stations. When compared in a slightly wider passband, from 0.03 to 0.3 Hz, a strong signal-generated noise can be observed at MOBB, but not on the land stations. The narrow-band character of the signal-generated noise is routinely observed in the MOBB P-wave data. An example of the signal-generated noise observed for the 459 km deep M_w 7.3 Kurile Islands earthquake of 17 November 2002 is also presented in Figure 10.

4. Background Noise Removal

4.1. Time-Domain, Frequency-Independent Method

[13] A simple method for the removal of the long-period noise is to subtract simultaneously recorded

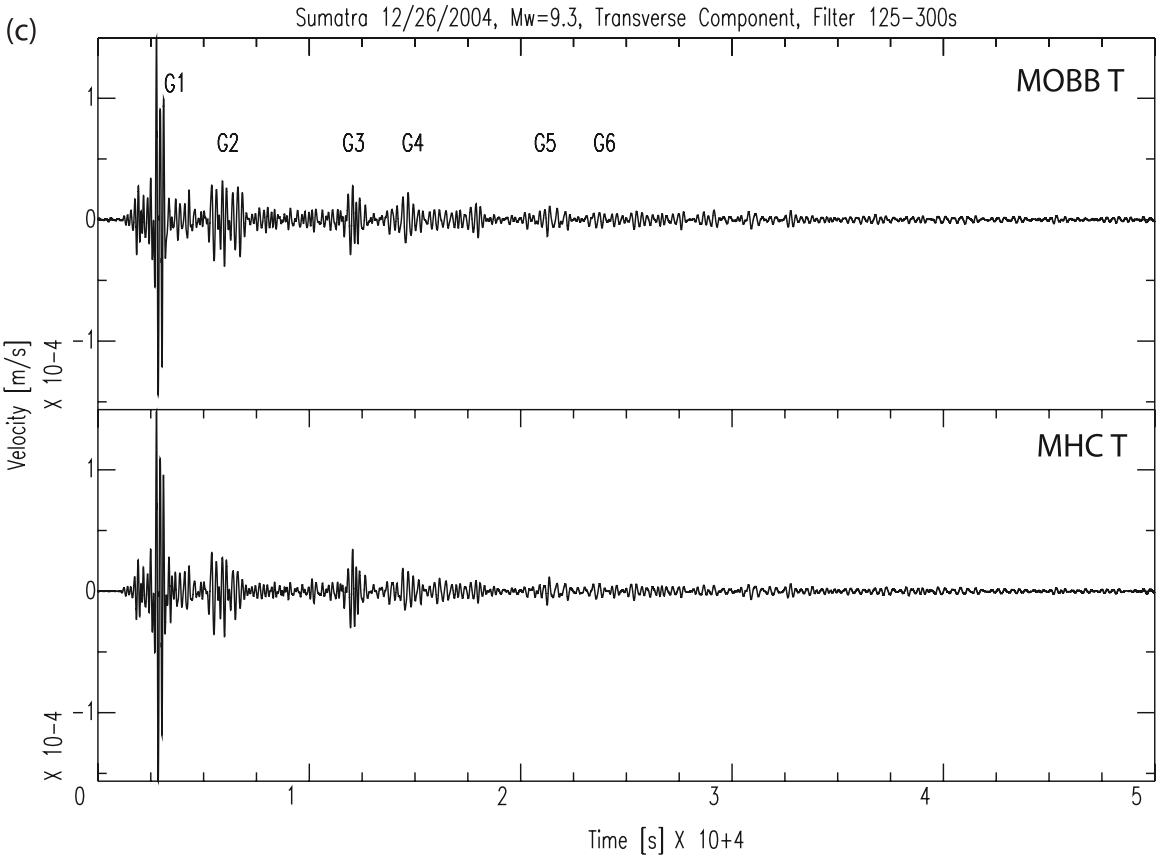

Figure 3. (continued)

ocean bottom pressure signal from the vertical seismic acceleration in time domain. The scale factor by which the pressure signal is multiplied is assumed to be frequency independent and is linearly estimated from the data. In the past, this method has been used to remove atmospheric pressure signal from the gravimeter observations made on land for earth tide studies [e.g., *Warburton and Goodkind*, 1977]. Later, it was proposed as a way to remove local barometric pressure signal from the vertical seismic data recorded at land stations [*Zürn and Widmer*, 1995].

[14] The results obtained with MOBB data show that this method can also be used to remove long-period background noise from ocean bottom seismic data. Figure 6 shows the result for a 5.5-hour period without earthquakes for which the pressure signal was removed from the vertical seismic acceleration signal in time domain. To illustrate the successful removal of the infragravity "hump," the result shown in Figure 6 is presented in the frequency domain. The only requirement for this method is that the pressure signal is locally recorded at the ocean bottom. The advantage of this approach is that it is very fast and easy to apply. An example of the time domain approach for a period that included the 6 December 2004 M_w 6.8 Hokkaido, Japan, event is shown in Figure 8c. The DPG signal was subtracted from the MOBB vertical acceleration signal in time domain and the result was band-pass filtered between 0.001 and 0.1 Hz.

4.2. Transfer Function Method

[15] In this method, the pressure observations are combined with measurements of the transfer function between vertical seismic and pressure recordings to predict the vertical component deformation signal. The predicted signal is then removed from the vertical seismic data in either frequency or time domain [*Webb and Crawford*, 1999; *Crawford and Webb*, 2000]. The transfer function is calculated from records during times without earthquakes. Since it is only a function of structure at the MOBB location, it does not change with time and can be applied to all data from this site. Figure 7 shows an

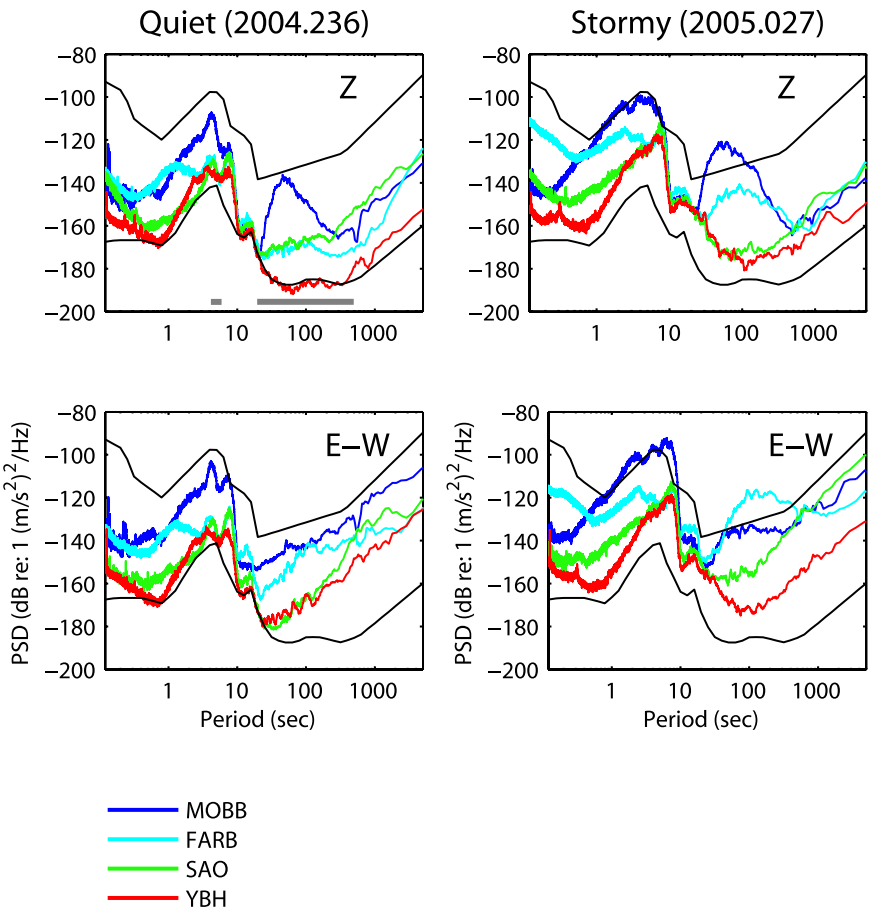

Figure 4. Comparison of the power spectral density (PSD) at the stations MOBB, FARB, SAO, and YBH calculated for a quiet day (2004, day 236) and for a stormy day (2005, day 027). Results obtained for the vertical (top) and for the horizontal components (E-W, bottom) are shown. The USGS high- and low-noise models for land stations are shown in black [*Peterson*, 1993]. The period bands for the signal-generated noise around 5 s and for the long-period noise from 20 to 500 s are shown as gray lines in the top left panel.

example of the transfer function method to remove noise from the earthquake free vertical MOBB data. The transfer function between the vertical seismic and the DPG signal was first calculated from 144 1-hour data windows within the 2005.034–056 interval (Figure 7b). The transfer function was then combined with pressure measurements for a 1-hour period on day 2005.035 to predict the vertical component deformation signal. This 1-hour period was not used in the transfer function calculation. The predicted deformation signal was then removed from the recorded vertical component data in frequency domain. The obtained result (Figure 7d) shows that most of the infragravity "hump" is removed. Also shown is coherence between the pressure and vertical seismic signal for the selected 1-hour period on day 2005.035 (Figure 7c). The method only works when coherence between the two channels used to compute the transfer function is high (almost 1) in the period band of interest (20 to 200 s). This means that the noise observed on the vertical seismic channel indeed results from the pressure signal. Low coherence would suggest that the observed noise comes from other sources (e.g., ocean currents).

[16] An example of the long-period background noise removal for a period that included an earthquake is shown in Figure 8. The 1-hour period used in the calculation now included the 6 December 2004 M_w 6.8 Hokkaido, Japan, event. The same transfer function as described above and shown in Figure 7b was used. The result shows that the method successfully recovers the seismic phases that were previously hidden by the long-period background noise. For this and other events we tried to "clean" the seismic signal of the long-

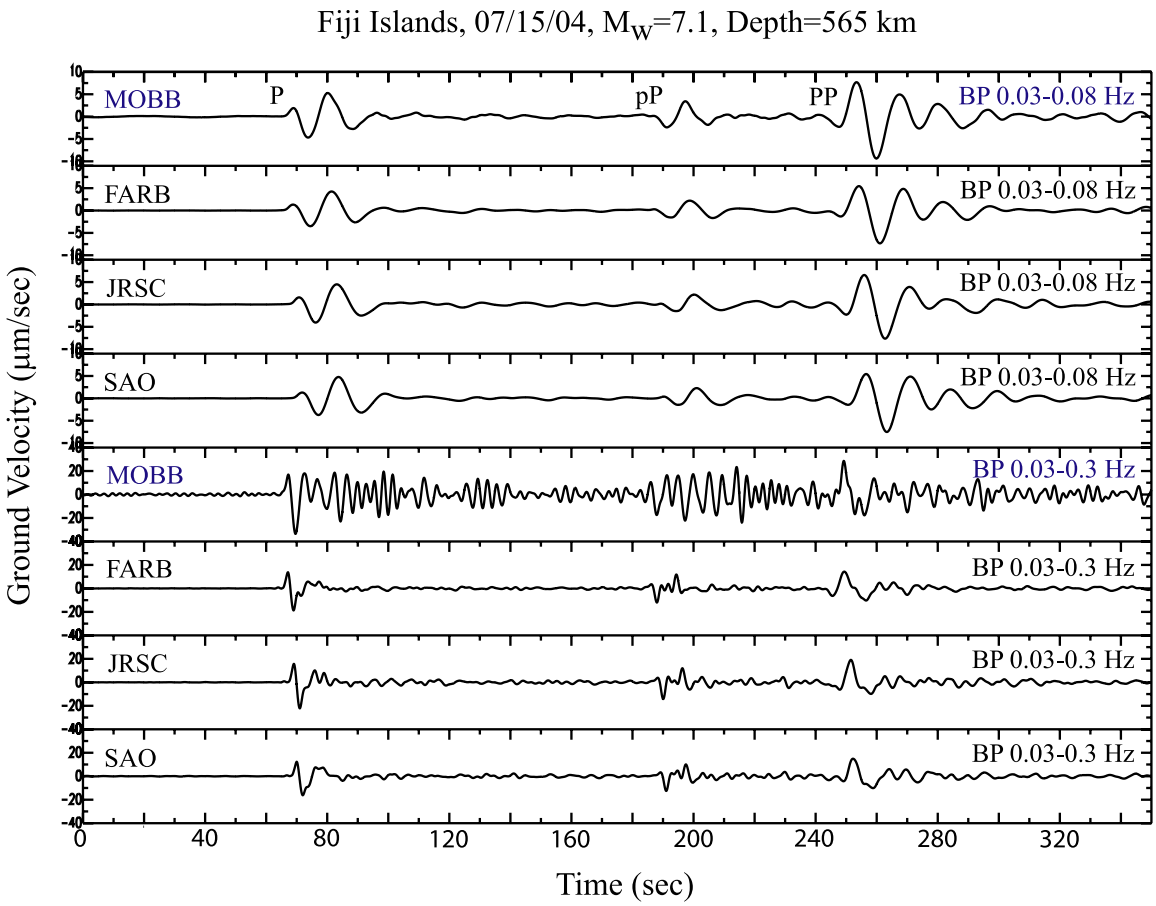

Figure 5. Comparison of the vertical component records at stations MOBB, FARB, JRSC, and SAO for the 565 km deep M_w 7.1 Fiji Islands earthquake of 15 July 2004. The data are shown in two passbands, 0.03–0.08 Hz and 0.03–0.3 Hz, to emphasize the narrow-band character of the signal-generated noise in the MOBB P-wave data. Clearly visible in the lower-frequency band are the P, pP, and PP arrivals.

period background noise by filtering only. Since the frequency of the observed teleseismic signal is within the frequency band of the observed long-period noise, the results obtained with the above described deconvolution method were always superior.

5. Signal-Generated Noise Removal

[17] Signal-generated noise due to reverberations of seismic waves in the shallow sedimentary layers may be unavoidable in buried ocean bottom installations. However, it can also be removed by post-processing, using either an empirical transfer function obtained from a nearby land station, or a synthetic transfer function obtained by modeling the response of the shallow structure at MOBB.

[18] In an empirical approach, the data from the nearby land station that does not show the signal-generated noise was used to obtain the transfer function between MOBB and a nearby land station. The 55 s long time window that included only the P wave was used in the calculation (see Figure 9a). To determine the transfer function, the instrument response was first removed and the data were deconvolved to ground displacement. Cross-correlation was then used to determine the time delays between the two stations. The P-wave arrival in the 0.03 to 0.1 Hz passband was used in computing the cross-correlation. The obtained time delay was applied to one of the records. The data to be used in the analysis were then filtered in the 0.03 to 0.3 Hz passband. The FFT (modulus, phase) was calculated for MOBB and the land station and the transfer function was obtained by spectral division of the MOBB and the land station results. A threshold of 0.01 of the absolute complex spectral amplitude was used to avoid division by a small number and still preserve the complex

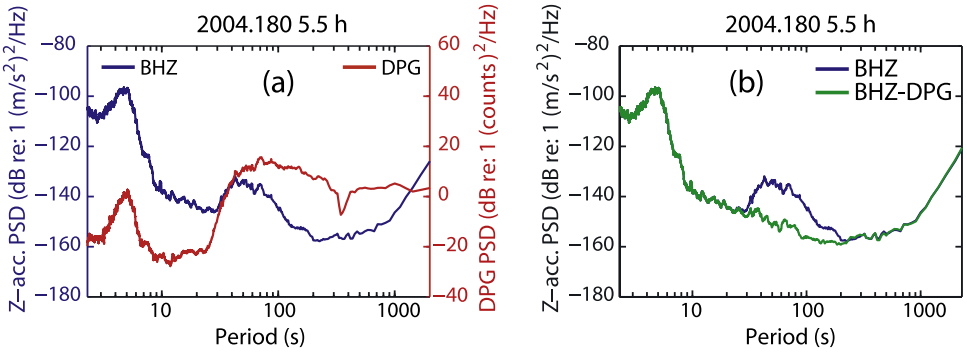

Figure 6. (a) Power spectral density (PSD) calculated for a 5.5-hour period without earthquakes for the vertical seismic channel (blue) and the DPG (red). At periods longer than 20 s the infragravity "hump" is observed for both data sets. (b) PSD for the vertical seismic channel before (blue) and after (green) the time domain subtraction of the DPG signal. Most of the infragravity "hump" is removed from the seismic data.

spectral phase information. Once we obtained the empirical transfer function, the signal-generated noise was removed from the MOBB data through deconvolution. Results obtained with this method for the Fiji Islands event from Figure 5 are presented in Figure 9c. Island station FARB was used as a reference land station to obtain the empirical transfer function. Results obtained with land stations SAO and JRSC as reference stations produced similar results. The same method was also used to remove the signal-generated noise from the Kurile Islands earthquake presented in Figure 10c. Again, the island station FARB was used as a reference land station. Results obtained with station JRSC used as a reference station are presented in Figure 13 of *Romanowicz et al.* [2006]. To demonstrate that the empirical transfer function from one event can be used to remove signal-generated noise from another other event, we used the empirical transfer function obtained from the Kurile event shown in Figure 10 to "clean" the Fiji Islands event data. The results in Figure 9d show that most of the signal-generated noise at MOBB was removed. This suggests that to routinely clean smaller events, we will not need to compute the empirical transfer function every time, but rather use one from a previous strong event. The fact that the empirical transfer function from the Kurile event (backazimuth from MOBB was 312°) worked well for the Fiji Islands event (backazimuth from MOBB was 235°) also shows that the empirical transfer function is not strongly azimuthally dependent.

[19] Instead of using the empirical transfer function, a synthetic transfer function can be obtained by 1-D modeling of the shallow structure. In this case the response of the sedimentary layers is modeled using the propagator matrix approach [*Kennett and Kerry*, 1979]. We used a program for a plane wave incident from below on a stack of layers (L. Johnson, personal communication, 2003). To obtain the response of the 1-D structure without a slow sedimentary layer, we used a previously published 1-D P-wave velocity crustal model for this region [*Begnaud et al.*, 2000]. Since the original model only includes P-wave velocities, we added the S-wave velocities by keeping the Poisson's ratio constant at 1.73. Similarly we obtained the densities from the P-wave velocities by using the Nafe-Drake relationship [*Brocher*, 2005]. The P-, S-wave velocity, and density profiles are shown in Figure 11. The top layer in this model is 1 km thick and has v_p = 2.87 km/s, v_s = 1.66 km/s, and ρ = 2.19 g/cm^3. We then modified this model by replacing the top 350 m with a slower sedimentary layer with v_p = 0.324 km/s, v_s = 0.196 km/s, and ρ = 1.3 g/cm^3, and calculated the response of the updated model. The thickness of the added sedimentary layer agrees with what is expected for the region of Smooth Ridge where MOBB was installed (sedimentary section less than 1 km total (R. Whitmarsh, personal communication, 2003)). The seismic velocities and density used for the added sedimentary layer were taken from the USGS velocity model [*Jachens et al.*, 1997] where they were assigned to the San Francisco Bay shallow sediments. The synthetic transfer function was obtained by the spectral division of the result obtained with the 1-D model with the additional sedimentary layer and the result obtained with the original 1-D crustal model. The synthetic transfer function was then used to decon-

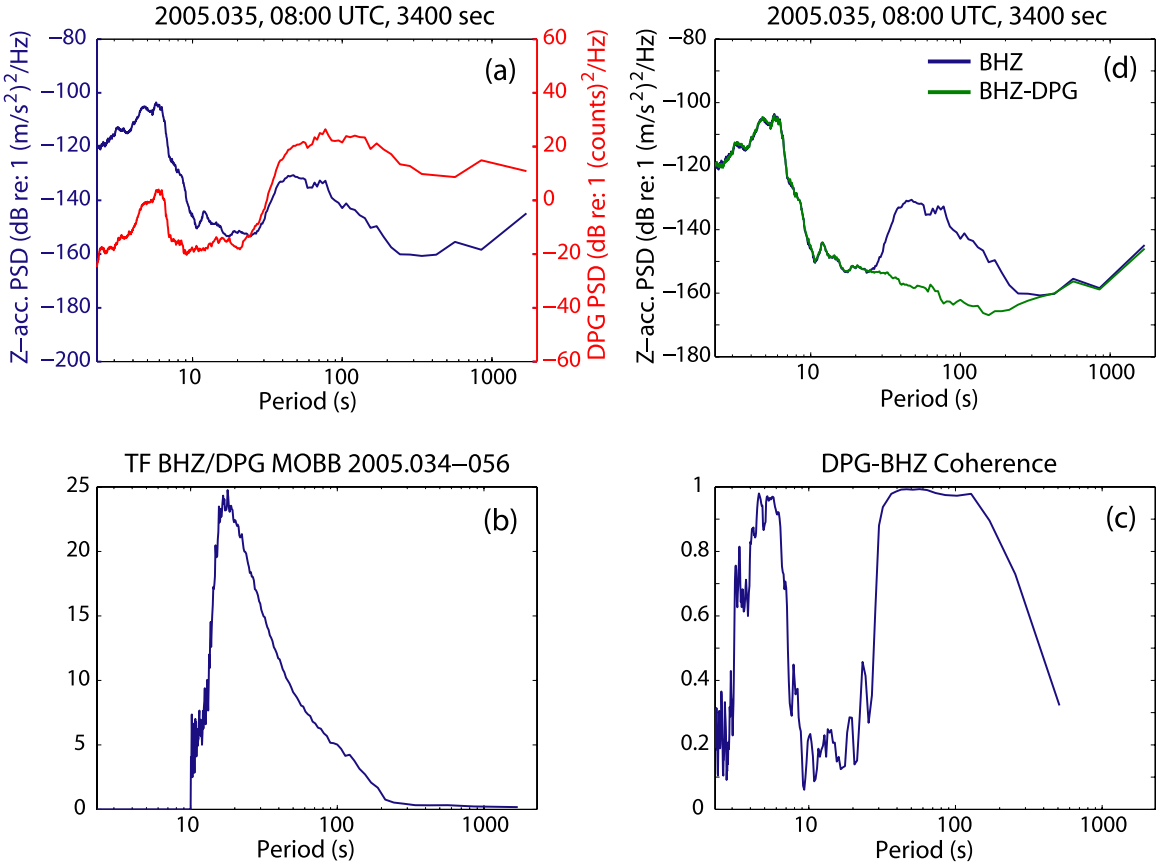

Figure 7. Example of the transfer function method to remove noise from the earthquake-free vertical data. (a) Power spectral density (PSD) for 1-hour period without earthquakes for the vertical seismic channel (blue) and DPG (red). (b) Transfer function between vertical seismic and DPG signal calculated from 144 1-hour-long data windows within the 2005.034–056 period. (c) Coherence between the vertical seismic and DPG channel for the selected 1-hour period. (d) PSD for the vertical seismic channel before (blue) and after (green) the noise removal using transfer function shown in Figure 7a.

volve the signal-generated noise from the MOBB vertical channel (Figures 9e and 10d). Results presented in Figures 9 and 10 show that both methods can successfully remove the signal-generated noise from the MOBB data and that the obtained results are similar to the waveforms observed at the nearby land station (Figures 9b and 10b).

[20] To test the stability of the synthetic deconvolution approach, we used the above described method with the transfer functions for slightly perturbed 1-D structures. The Kurile Islands event from Figure 10 was used in this analysis. Results obtained with 25 different 1-D models are shown in Figure 12. The top layer thickness of the models varied from 250 m to 450 m and the top layer seismic velocities were changed for up to 20% from the above used sedimentary layer values. Since small perturbations in density result in waveform changes that are much smaller than when the seismic velocities are perturbed, we only explored the velocity perturbations and kept the density of the sedimentary layer constant. The misfit between the cleaned MOBB and FARB waveforms was evaluated by the variance reduction that is listed in each panel. The central panel corresponds to the model described above and presented in Figure 10d. The results show that models with a slightly thicker and faster, as well as slightly thinner and slower top layer also remove a significant portion of the observed signal-generated noise at MOBB. The model with a 350 m thick top layer used in Figure 10d remained the favorite model as, in addition to a large variance reduction, it also resulted in good agreement of the amplitudes of the strongest seismic phases observed at FARB and cleaned MOBB records. Figure 13 shows a similar analysis

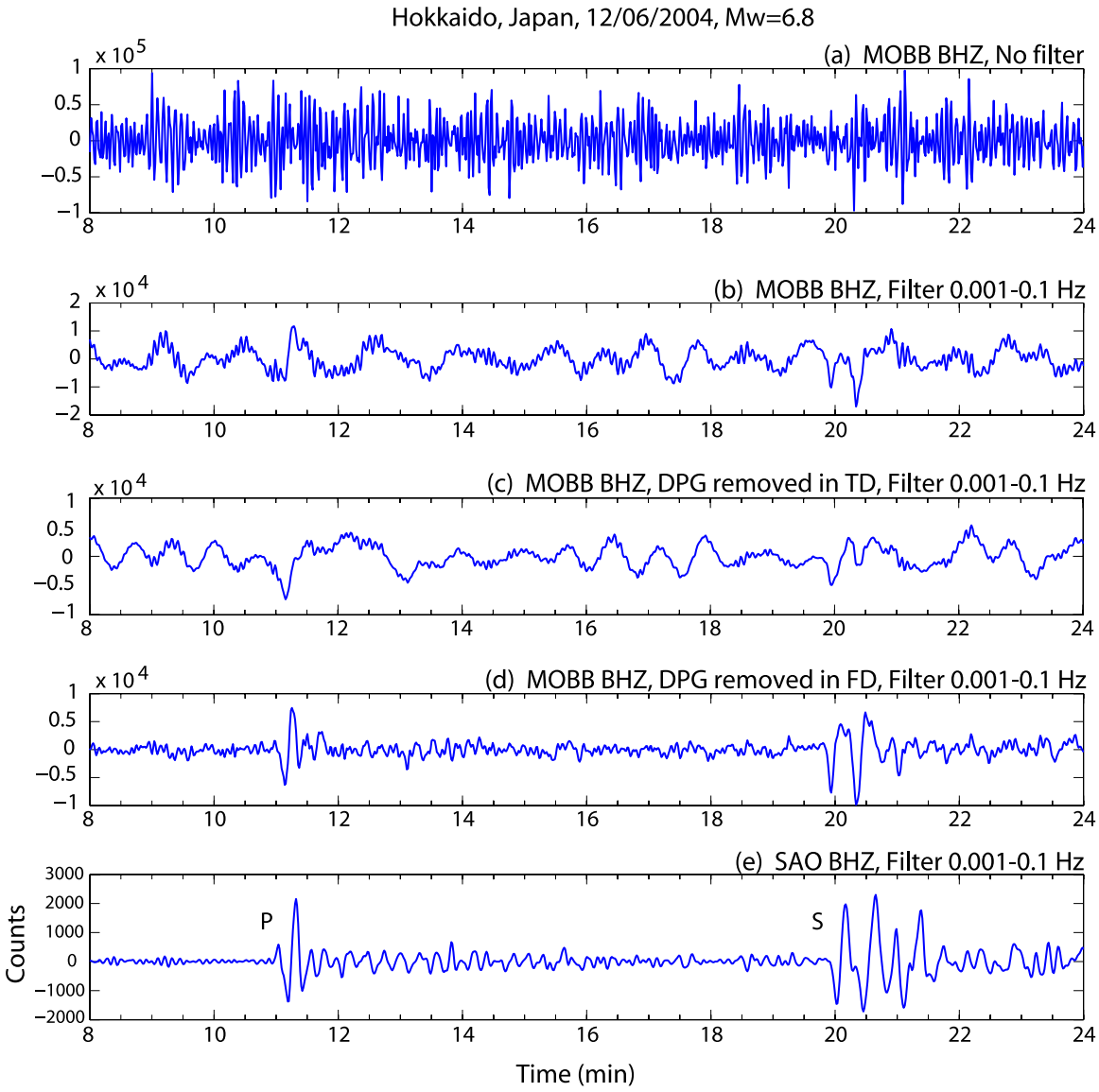

Figure 8. Example of long-period background noise removal for the 6 December 2004 M_w 6.8 Hokkaido, Japan, earthquake using the transfer function shown in Figure 7b. (a) Original MOBB vertical data. (b) MOBB data band-pass filtered between 0.001 and 0.1 Hz. (c) MOBB data after subtraction of the DPG signal in time domain and band-pass filtered between 0.001 and 0.1 Hz. (d) MOBB data after removal of the coherent DPG signal and band-pass filtered between 0.001 and 0.1 Hz. (e) SAO data band-pass filtered between 0.001 and 0.1 Hz.

as presented in Figure 12, but now for the Fiji Islands event from Figure 9. The top layer thickness of the models again varied from 250 m to 450 m and the top layer seismic velocities used in Figure 10d were changed by up to 20%. Listed in each panel is the variance reduction. The results show that a thinner and slightly faster layer (250 m, 10% faster top layer velocity; shown in the first column, second row) better removes the signal-generated noise from the MOBB record than the 1-D model that worked best for the Kurile Islands event (panel in the center). It is possible that the layered structure at MOBB is slightly tilted and that the 1-D structure therefore appears different for the event coming from a different azimuth.

6. Discussion

[21] The described methods are an important tool to remove noise from the seismic data recorded at

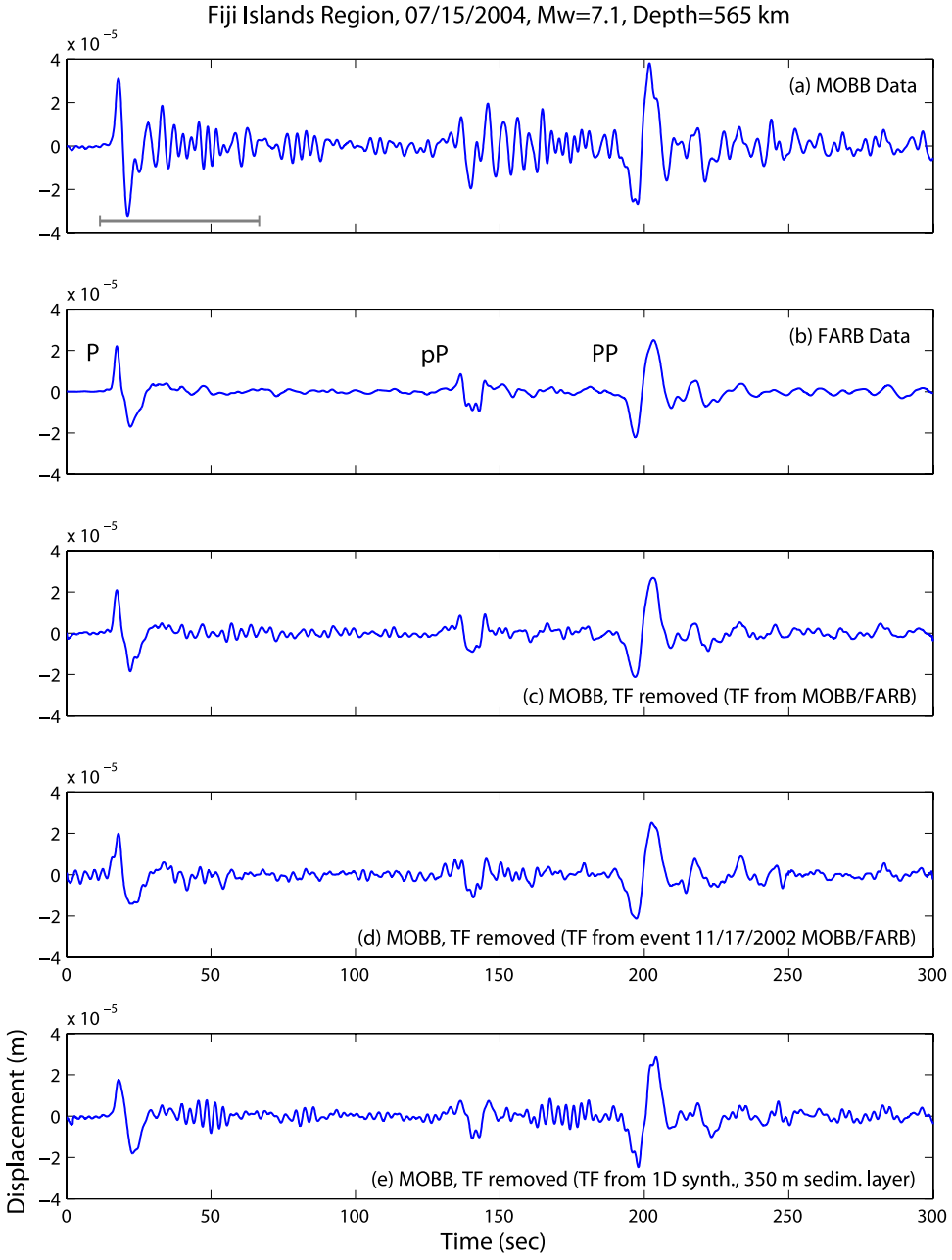

Figure 9. Two examples of deconvolution of the signal-generated noise at MOBB for the Fiji Islands event shown in Figure 5. (a) Original MOBB data. The time window used in the transfer function calculation is indicated. (b) Original FARB data. (c) MOBB data after removing empirical transfer function constructed using MOBB and FARB data. (d) Same as Figure 9c, only that empirical transfer function obtained from the Kurile Islands event shown in Figure 10 was used. (e) MOBB data after removing a synthetic transfer function obtained by 1-D modeling of the shallow structure with a 350 m sedimentary layer with v_p = 0.324 km/s, v_s = 0.196 km/s, and ρ = 1.3 g/cm^3.

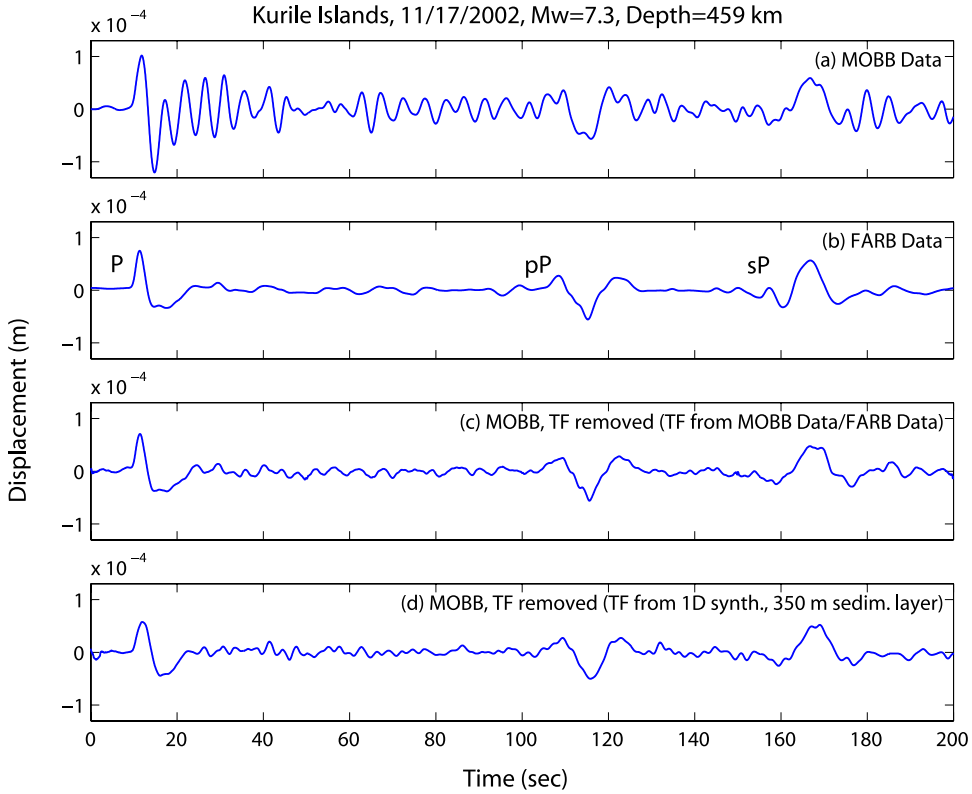

Figure 10. Two examples of deconvolution of the signal-generated noise at MOBB for the 17 November 2002 M_w 7.3 Kurile Islands event. (a) Original MOBB data. (b) Original FARB data. (c) MOBB data after removing empirical transfer function constructed using MOBB and FARB data. (d) MOBB data after removing a synthetic transfer function obtained by 1-D modeling of the shallow structure with a 350 m layer with v_p = 0.324 km/s, v_s = 0.196 km/s, and ρ = 1.3 g/cm^3.

ocean bottom buried broadband installations. Both methods used to remove the long-period background noise require the locally recorded pressure signal at the seafloor. It is therefore extremely important to have a reliable pressure sensor collocated with every ocean bottom seismometer. It is also important that the sampling rate for the DPG and other environmental data (e.g., temperature, ocean current speed and direction) is high enough so that they can be used in the postprocessing for the complete seismic frequency band.

[22] Other studies [*Crawford and Webb*, 2000; *Stutzmann et al.*, 2001] suggest that tilt-generated seismic background noise due to ocean currents can also be an important noise source for seismic instruments that are not well leveled. Current-induced tilt noise is mainly caused by seafloor currents flowing past the instrument and by eddies spun off the back of the instrument [*Webb*, 1988; *Duennebier and Sutton*, 1995]. The MOBB sensor is buried below the seafloor and was well leveled during the installation; therefore the tilt noise

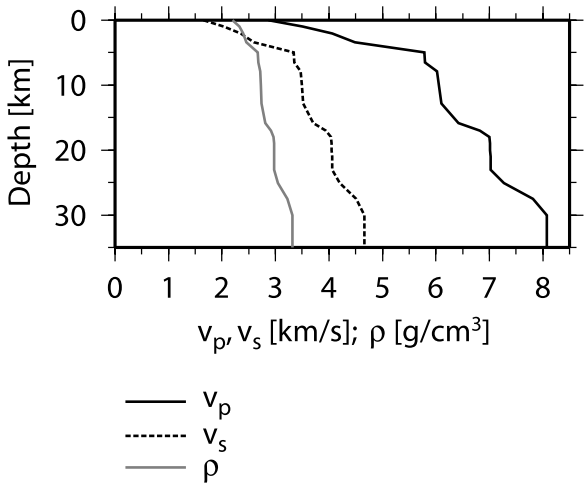

Figure 11. The P- and S-wave velocity and density profiles for the original 1-D crustal model based on the results from *Begnaud et al.* [2000].

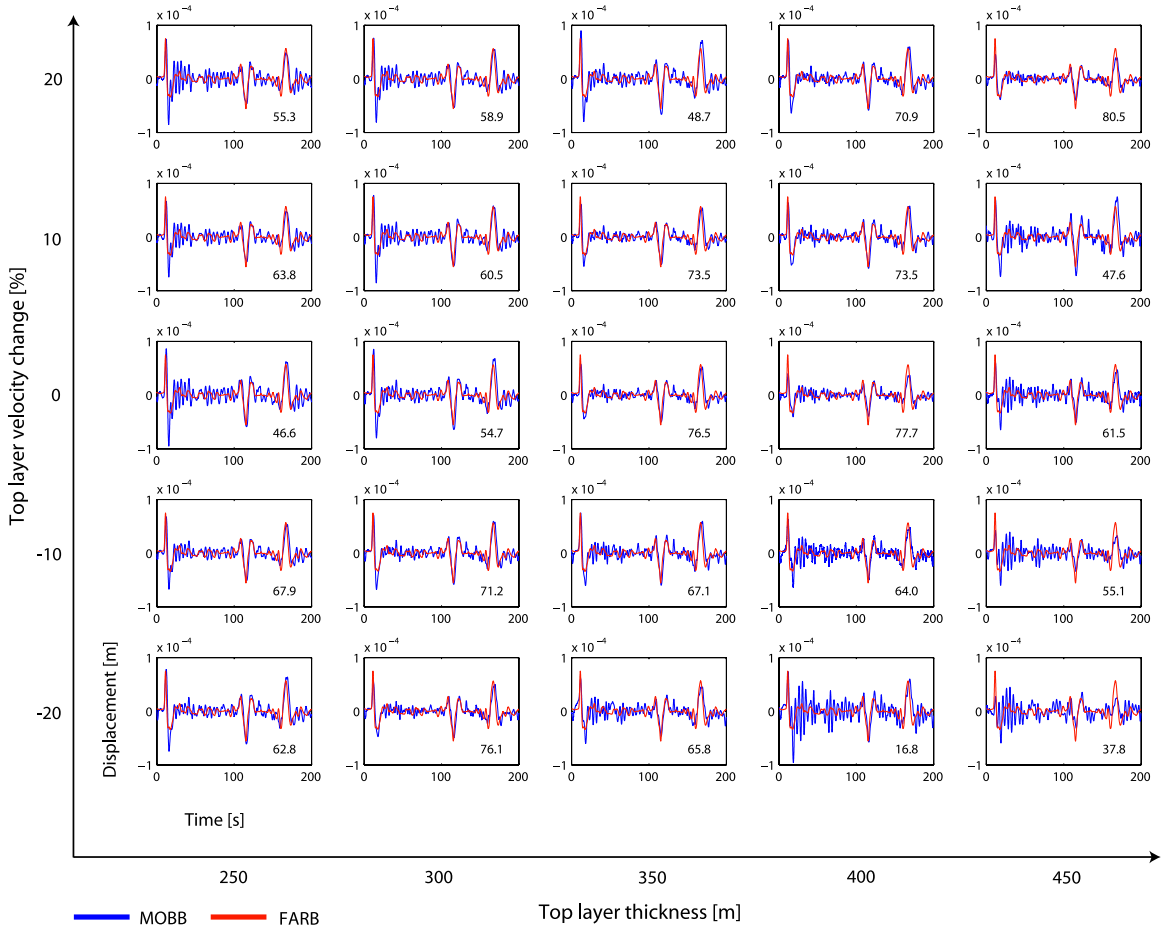

Figure 12. Deconvolution of signal-generated noise at MOBB for the Kurile Islands event shown in Figure 10. The MOBB data after removing a synthetic transfer function are compared to observations at FARB. Results obtained with the transfer functions calculated for 25 different 1-D models are shown. Models varied in the top layer thickness and the top layer seismic velocities. The top layer seismic velocities used in Figure 10d were changed by up to 20%. Listed in each panel is the variance reduction.

should not be significant. Additional analysis of the MOBB data confirms that coherence between the noise recorded on the vertical and horizontal channels is low. We applied the same technique as described above to remove the pressure signal from the vertical data, but this time using the horizontal and vertical channels. We first computed the transfer function between horizontal and vertical channels and then subtracted the predicted vertical deformation from the observed vertical signal. The results showed that there is almost no improvement, suggesting that the tilt noise is not important at MOBB.

[23] We plan to further investigate coherence between vertical and horizontal seismic channels, as well as coherence between the seismic channels and other measured environmental variables such as temperature and current flow that are also measured at MOBB. In case high coherence between any of the above observables and either of the seismic channels is observed, we will use it to further clean the seismic data. We will also further test the stability of the transfer function between pressure and vertical seismic channel and set up an automatic routine that will remove noise from the MOBB vertical seismic channel. Once MOBB is connected to the cable, this type of processing can be performed in real time.

[24] The long-period background noise can also be used to determine the density and elastic parameters of the oceanic crust and upper mantle below the station [e.g., *Crawford et al.*, 1991, 1998]. In our future work we plan to use the seafloor compliance inversion to determine the shear veloc-

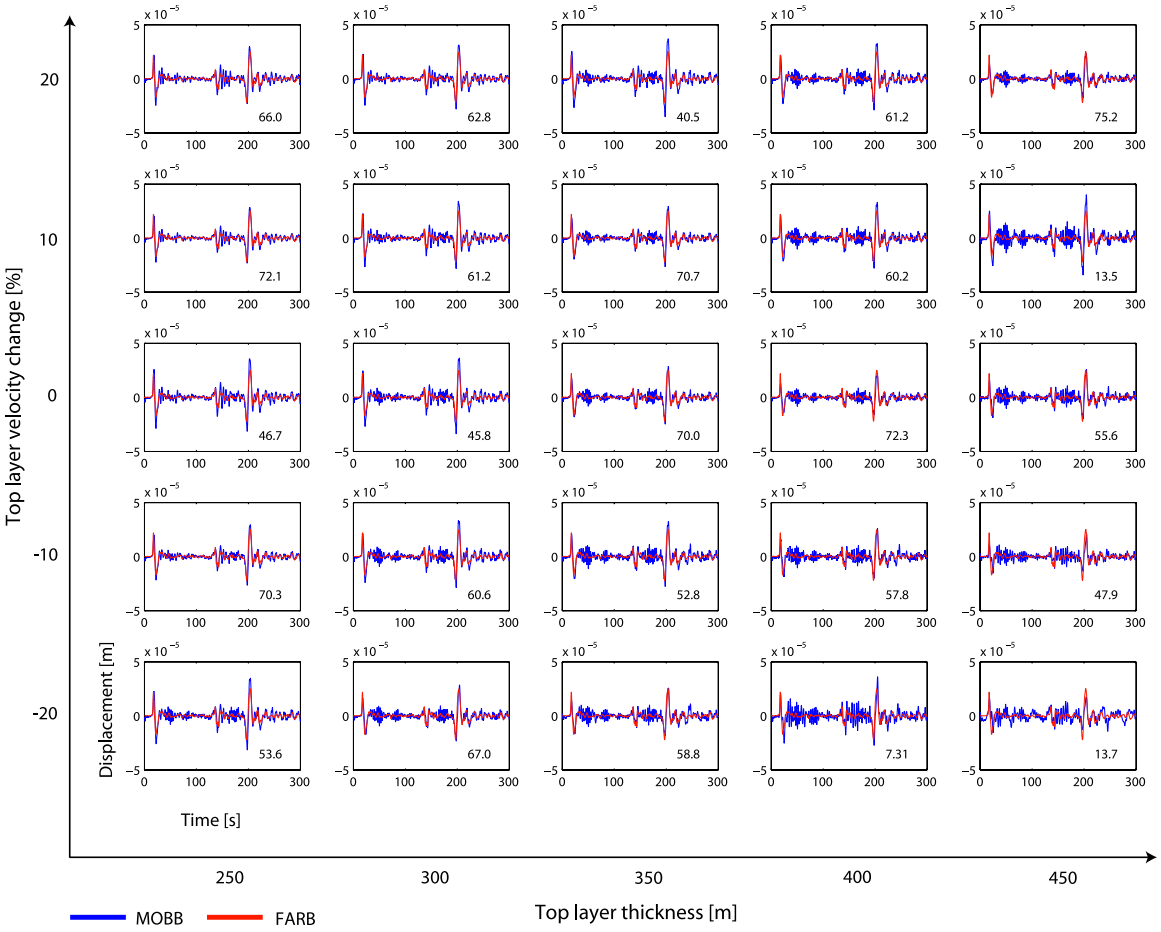

Figure 13. Deconvolution of signal-generated noise at MOBB for the Fiji Islands event shown in Figure 9. The MOBB data after removing a synthetic transfer function are compared to observations at FARB. Results obtained with the transfer functions calculated for 25 different 1-D models are shown. Models varied in the top layer thickness and the top layer seismic velocities. The top layer seismic velocities used in Figure 10d were changed by up to 20%. Listed in each panel is the variance reduction.

ity structure of the oceanic crust below the Smooth Ridge region of the Monterey Bay.

Acknowledgments

[25] The MOBB instrumentation, deployment, and maintenance were supported by Lucile and David Packard Foundation funds to MBARI, NSF grant OCE9911392, and UC Berkeley funds. This is contribution 06-13 of the UC Berkeley Seismological Laboratory.

References

Araki, E., M. Shinohara, S. Sacks, A. Linde, T. Kanazawa, H. Shiobara, H. Mikada, and K. Suyehiro (2004), Improvement of seismic observation in the ocean by use of seafloor boreholes, *Bull. Seismol. Soc. Am.*, *94*, 678–690.

Begnaud, M. L., K. C. McNally, D. S. Stakes, and V. A. Gallardo (2000), A crustal velocity model for locating earthquakes in Monterey Bay, California, *Bull. Seismol. Soc. Am.*, *90*, 1391–1408.

Brocher, T. M. (2005), Empirical relations between elastic wavespeeds and density in the Earth's crust, *Bull. Seismol. Soc. Am.*, *95*, 2081–2092.

Cox, C., T. Deaton, and S. Webb (1984), A deep-sea differential pressure gauge, *J. Atmos. Oceanic Technol.*, *1*, 237–246.

Crawford, W. C., and S. C. Webb (2000), Identifying and removing tilt noise from low-frequency (<0.1 Hz) seafloor vertical seismic data, *Bull. Seismol. Soc. Am.*, *90*, 952–963.

Crawford, W. C., S. C. Webb, and J. A. Hildebrand (1991), Seafloor compliance observed by long-period pressure and displacement measurements, *J. Geophys. Res.*, *96*, 16,151–16,160.

Crawford, W. C., S. C. Webb, and J. A. Hildebrand (1998), Estimating shear velocities in the oceanic crust from compliance measurements by two-dimensional finite difference modeling, *J. Geophys. Res.*, *103*, 9895–9916.

Dolenc, D. (2006), Results from two studies in seismology: I. Seismic observations and modeling in the Santa Clara Valley, California; II. Observations and removal of the long-period noise at the Monterey Ocean Bottom Broadband seismic station (MOBB), Ph.D. thesis, Univ. of Calif., Berkeley.

Dolenc, D., B. Romanowicz, D. Stakes, P. McGill, and D. Neuhauser (2005), Observations of infragravity waves at the Monterey Ocean Bottom Broadband station (MOBB), *Geochem. Geophys. Geosyst.*, *6*, Q09002, doi:10.1029/2005GC000988.

Duennebier, J. K., and G. H. Sutton (1995), Fidelity of ocean bottom seismic observations, *Mar. Geophys. Res.*, *17*, 535–555.

Jachens, R. C., R. F. Sikora, E. E. Brabb, C. M. Wentworth, T. M. Brocher, M. S. Marlow, and C. W. Roberts (1997), The basement interface: San Francisco Bay area, California, 3-D seismic velocity model, *Eos Trans. AGU*, *78*(46), Fall Meet. Suppl., F436.

Kennett, B. L. N., and N. J. Kerry (1979), Seismic waves in a stratified half space, *Geophys. J. R. Astron. Soc.*, *57*, 557–583.

Kinsman, B. (1984), *Wind Waves: Their Generation and Propagation on the Ocean Surface*, 676 pp., Prentice-Hall, Upper Saddle River, N. J.

McGill, P., D. Neuhauser, D. Stakes, B. Romanowicz, T. Ramirez, and R. Uhrhammer (2002), Deployment of a long-term broadband seafloor observatory in Monterey Bay, *Eos Trans. AGU*, *83*(47), Fall Meet. Suppl., Abstract F1008.

Peterson, J. (1993), Observations and modeling of seismic background noise, *U.S. Geol. Surv. Tech. Rep.*, *93-322*, 95 pp..

Romanowicz, B., et al. (1998), MOISE: A pilot experiment towards long term sea-floor geophysical observatories, *Earth Planets Space*, *50*, 927–937.

Romanowicz, B., D. Stakes, R. Uhrhammer, P. McGill, D. Neuhauser, T. Ramirez, and D. Dolenc (2003), The MOBB Experiment: A prototype permanent off-shore ocean bottom broadband station, *Eos Trans. AGU*, *84*(34), 325, 331–332.

Romanowicz, B., D. Stakes, D. Dolenc, D. Neuhauser, P. McGill, R. Uhrhammer, and T. Ramirez (2006), The Monterey Bay Broadband Ocean bottom seismic observatory, *Ann. Geophys.*, *49*, 607–623.

Stephen, R. A., F. N. Spiess, J. A. Collins, J. A. Hildebrand, J. A. Orcutt, K. R. Peal, F. L. Vernon, and F. B. Wooding (2003), Ocean Seismic Network Pilot Experiment, *Geochem. Geophys. Geosyst.*, *4*(10), 1092, doi:10.1029/2002GC000485.

Stutzmann, E., et al. (2001), MOISE: A prototype multiparameter ocean-bottom station, *Bull. Seismol. Soc. Am.*, *91*, 885–892.

Sutton, G. H., F. K. Duennebier, and B. Iwataki (1981), Coupling of ocean bottom seismometers to soft bottom, *Mar. Geophys. Res.*, *5*, 35–51.

Uhrhammer, R., B. Romanowicz, D. Neuhauser, D. Stakes, P. McGill, and T. Ramirez (2002), Instrument testing and first results from the MOBB Observatory, *Eos Trans. AGU*, *83*(47), Fall Meet. Suppl., Abstract F1008.

Uhrhammer, R. A., D. Dolenc, B. Romanowicz, D. Stakes, P. McGill, D. Neuhauser, and T. Ramirez (2003), MOBB: Data analysis from an ocean floor broadband seismic observatory, *Eos Trans., AGU*, *84*(46), Fall Meet. Suppl., Abstract F1137.

Warburton, R. J., and J. M. Goodkind (1977), The influence of barometric pressure variations on gravity, *Geophys. J. R. Astron. Soc.*, *48*, 281–292.

Webb, S. C. (1988), Long-period acoustic and seismic measurements and ocean floor currents, *IEEE J. Oceanic Eng.*, *13*, 263–270.

Webb, S. C. (1998), Broadband seismology and noise under the ocean, *Rev. Geophys.*, *36*, 105–142.

Webb, S. C., and W. C. Crawford (1999), Long-period seafloor seismology and deformation under ocean waves, *Bull. Seismol. Soc. Am.*, *89*, 1535–1542.

Zürn, W., and R. Widmer (1995), On noise reduction in vertical seismic records below 2 mHz using local barometric pressure, *Geophys. Res. Lett.*, *22*, 3537–3540.